

Electrical power generation from piezoelectric electrospun nanofibers membranes: electrospinning parameters optimization and effect of membranes thickness on output electrical voltage

Ali Gheibi · Roohollah Bagherzadeh · Ali Akbar Merati · Masoud Latifi

Received: 17 June 2014 / Accepted: 21 September 2014 / Published online: 3 October 2014
© Springer Science+Business Media Dordrecht 2014

Abstract Nanogenerators based on piezoelectric nanofibers capable to scavenging mechanical energy from the environment and converting into usable electrical energy. In this research work, the electrospinning parameters were optimized to produce randomly oriented uniform PVDF nanofiber mats without structural defects. Then, optimized nanofiber membranes with different thickness (110, 220, and 310 μm) were fabricated and their output voltages as a performance factor of the nanogenerator were measured. Results indicated that the nanogenerator based on piezoelectric nanofibers can generate voltage as high as several volts electrical outputs by applying mechanical impact. Finally, to investigate the effect of pure thickness on power harvesting efficiency, output voltages of samples were normalized to thickness. Results showed that in spite of the existed literature, increases in nanofiber membrane's thickness can lead to decrease the output voltage of nanogenerator. These results imply promising applications for various wearable self-powered electrical devices within the clothing systems.

Keywords Nanogenerator · Piezoelectric nanofibers · Electrospinning · Output voltage · Wearable electronic

Introduction

Due to recent years, the growth in development and progress in electronic miniature, portable and flexible devices for applications such as control and monitoring health human and structure, military and industrial is rapid [1–6]. Producing a flexible, lightweight, versatile and very small self-powering source for this device is still far from the reality [4, 5, 7–11]. Piezoelectric polymers are suitable for produce self-powering flexible and lightweight sources. Since they can easily deform by small forces through tensile, mechanical impact, vibration mechanical, bending and pressure, they are a choice for self-powering of the microelectronic devices and also wearable electronics. They also possess high operating field strength and high dielectric breakdown, which means that they can withstand much higher driving fields than ceramics [4, 7, 12, 13].

Among piezoelectric polymers, Poly(vinylidene fluoride) (PVDF) and its copolymers have excellent piezoelectric properties [14–17]. The PVDF is a semi-crystalline polymer known by its polymorphism, depending on the processing conditions four different crystal structures: α , β , γ and σ can be obtained [18, 19]. However, only the β -phase has the best piezoelectric properties [8, 10, 18, 20, 21]. Although the inorganic nanowire-based electrical generators can be utilized over a wide working frequency range, they are required precisely controlled fabricating conditions. Furthermore, they are brittle and have a very limited strain level which limited their application. Piezoelectric polymer nanofibres, on the other hand, have much better flexibility and possess large sensitive areas. It is also demonstrated that fiber based generators have higher flexibility and lower weight compared to those made of thin films. They are mostly produced by electrospinning [8, 10, 18, 22, 23]. Applied high voltage or high stretching ratio of the polymer solution's jet in

A. Gheibi · M. Latifi
Textile Engineering Department, Textile Research and Excellence Centers, Amirkabir University of Technology, Tehran, Iran

R. Bagherzadeh (✉) · A. A. Merati
Advanced Textile Materials and Technology (ATMT) Research Institute, Amirkabir University of Technology, Tehran, Iran
e-mail: bagherzadeh_r@aut.ac.ir

Table 1 Different conditions used to optimize the electrospun micro-nanofibers

Sample No.	Volumetric ratio (Acetone/DMF)	Concentration (wt.%)	TCD* (cm)	Flow rate (ml/h)	Applied Voltage (kV)	Result
1	4/6	10	15	1	10.5	Non-uniform Fiber with bead
2			12	0.5	15	
3			15	0.5	15	
4			15	0.5	17	
5	14	14	15	0.5	17	
6			12	0.5	17	
7			15	0.5	15	
8			17	0.5	17	
9	17	17	10	0.5	17	
10			20	0.5	13	
11			15	0.5	11.5	
12			15	0.5	16	
13	2/8	20	15	0.5	14	
14			15	0.5	16	
15	4/6	23	15	0.5	17	
16			15	0.5	20	
17	26	26	15	0.5	15	uniform Fiber without defect (bead)
18			15	0.5	15	
19			15	0.5	20	
20	30	30	15	0.5	16	Uniform and thick Fiber without bead
21			15	0.5	18	

* Tip to Collector Distance

electrospinning process also benefits crystallization in the β phase without any further post treatments needed. Also alignment of the electrospun nanofibers by using a rotating collector can improve the formation of the β phase in the fibrous structure [18]. Both near field electrospinning and far field electrospinning techniques have been successfully used for making single and mats of poly(vinylidene fluoride) (PVDF) nanofiber, respectively. Both near field and far field electrospun PVDF nanofibers were directly used for making power generators without additional post treatments for to poling the dipoles within the fiber crystalline structure, which is an interesting benefit of using these techniques to make polymeric nanogenerators [8, 10, 17]. Single poly(vinylidene fluoride) (PVDF) nanofiber

prepared by a near field electrospinning technique have been used in order to make piezoelectric power generators [8, 17, 24, 25]. Zheng et al. [19] fabricated single poly(vinylidene fluoride) (PVDF) nanofiber prepared by a near field electrospinning technique and found that electrospinning with high evaporation rate for the solvent can effectively improve the formation of the desired phase (β phase) in the fiber structure for power generation application. It is well documented that the crystallinity structure, the β phase content, and the morphology are the key and important issues for making the nanofibers mats as a nanogenerator [18].

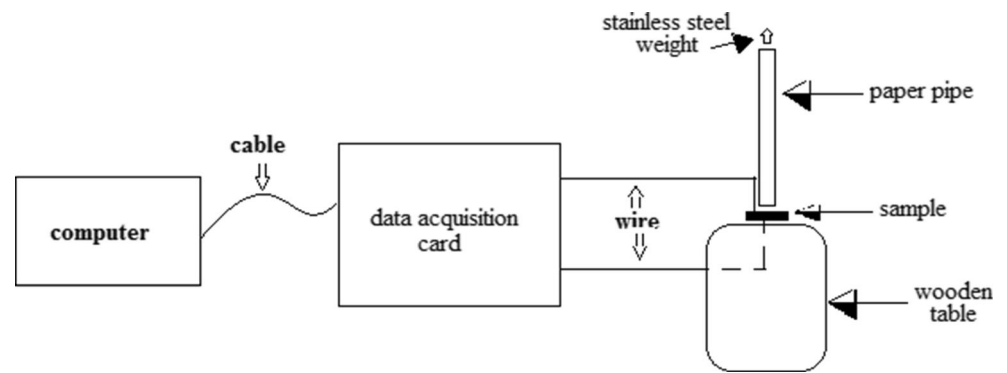
Although the feasibility of harvesting the energy from the PVDF membranes are investigated in the literature, the effect of different structural properties of electrospun PVDF nanofiber membranes should be scrutinized. Because of the critical dependence on residual charges on the fibers in the gap between the nanofiber device and conductive electrodes, it is hard to make a device with the requirements of a realistic device. Incorporating the output electrodes within the structure of the nanofibers mats during the electrospinning process is another requirement of making an effective wearable device. Therefore, in order to overcome the drawbacks of the

Table 2 Optimized conditions used to fabricate the electrospun nanofibrous nanogenerators

TCD (cm)	Flow rate (ml/h)	Applied Voltage (kV)	Volumetric ratio (Acetone/DMF)	CRS* (rpm)	Concentration (wt.%)
15	0.5	20	4/6	216	26

* Collector rotational speed

Fig. 1 Schematic of the setup used for evaluation of power generation of samples



existing devices, in this work, the electrospinning parameters were optimized in order to produce uniform randomly oriented PVDF nanofiber mats without structural defects and both nanofiber membrane and conductive electrodes were assembled simultaneously during the electrospinning process. Also, in order to study the effect of the membrane thickness on the output voltage of the nanogenerator, different samples with different thickness were produced and their output voltage as a performance factor of the nanogenerator were measured. Finally, output voltage of samples was normalized to the membrane's thickness to investigate the effect of pure thickness on their power harvesting efficiency.

Experimental

Materials

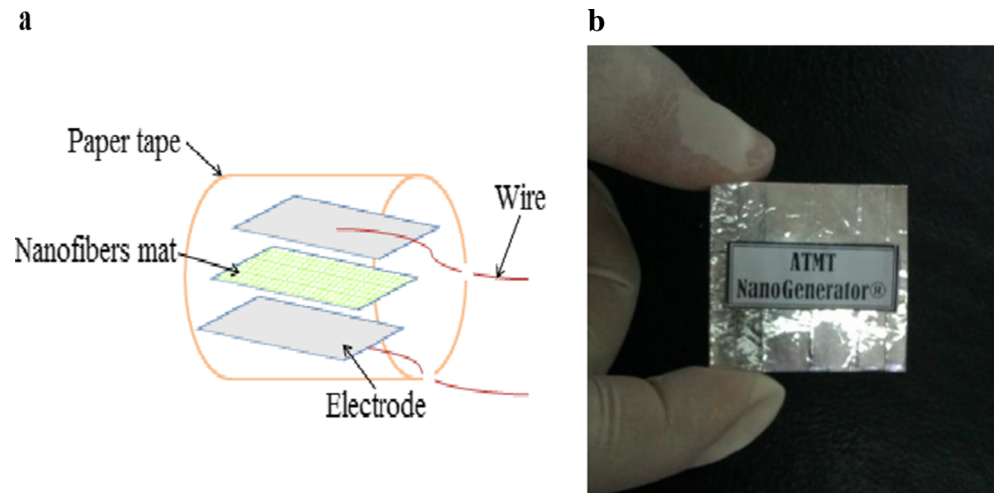
Poly(vinylidene fluoride) (PVDF) pellets with molecular weight viscosity of 46,000 (g.mol⁻¹) were purchased from Sigma-Aldrich. The solvents used in this work were N, N-

dimethylformamide (DMF, Merck Chem. Co.) and acetone (Merck Chem. Co.). All the materials were used without further purification.

Preparation of the PVDF Nanofibers membranes

A factorial experiment was designed to investigate the significance of processing parameters including polymer concentration, applied voltage, feed rate of polymer solution, collector rotation speed and electrospinning distance on average fiber diameter and morphology of nanofibers (Table 1). Extensive electrospinning experiments were performed accordingly and their morphologies, crystallinity, and mechanically robustness were compared in order to optimize the electrospinning and the solution parameters to formation of continuous, smooth fibers at high densities and with mesoscopic joints at crossing points. By comparing the initial results, the conditions are given in Table 2 was selected as the optimum conditions for fabrication of the device. Electrospinning was performed by a 1.0 ml plastic syringe tipped with a 22-gauge stainless steel needle. The positive lead from a high voltage supply (Gamma High

Fig. 2 **a** Schematic structure, and **b** photo of an actual of the nanofibrous generator device



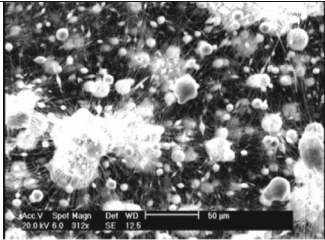
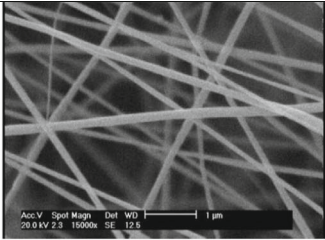
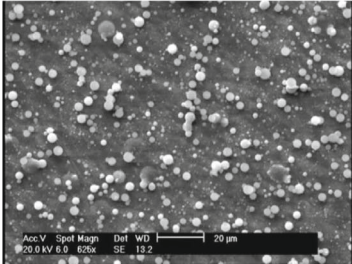
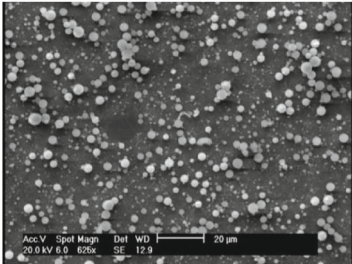
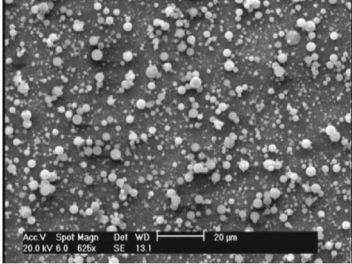
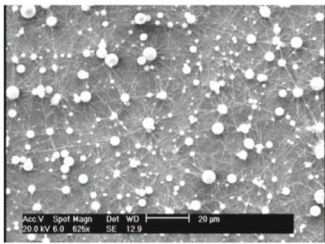
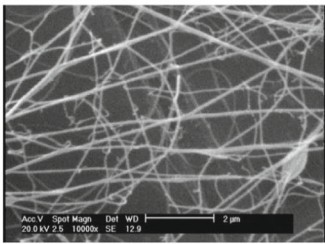
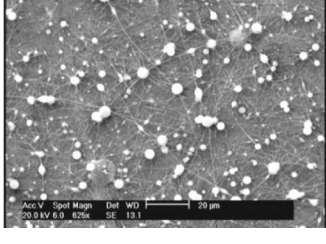
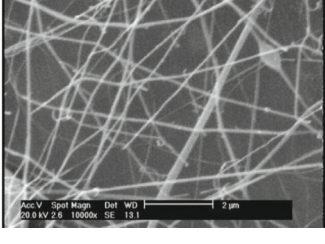
Sample No.	SEM images		Mean \pm Std of fiber diameter (nm)
	Scale 1	Scale 2	
1			110 \pm 39
2			No fiber
3			No fiber
4			No fiber
5			90 \pm 20
6			94 \pm 23

Fig. 3 SEM images and mean fiber diameters for PVDF nanofiber samples (according to conditions in Table 1)

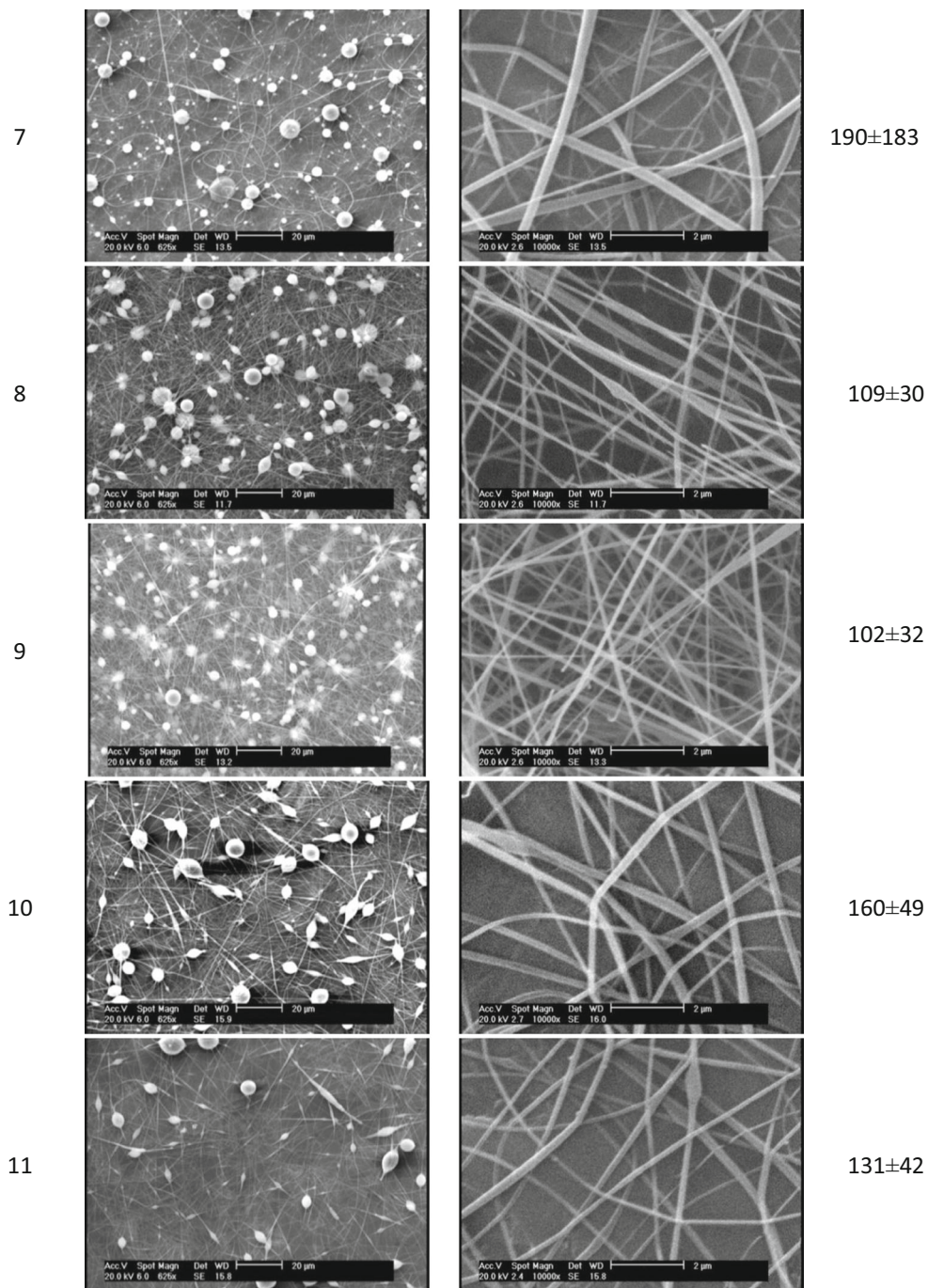


Fig. 3 (continued)

Voltage Research) connected to the metal needle, with the applied voltage of 20 kV. The solutions were injected into the needle at a constant rate of 0.5 ml/h with a syringe pump (KD Scientific, USA). A cylindrical drum collector (outer diameter 26 cm) wrapped with Cu foil, with some modification to be able to put the conductive electrodes on it during the electrospinning, were used as the collector [23]. The distance between

the needle tip and the collector was 15 cm, and rotational speed of collector was 180 rpm.

Preparation of PVDF film

A thin PVDF film sample, as the control sample, obtained from the spreading polymer solution on the glass and drying in an oven at the temperature 110 °C.

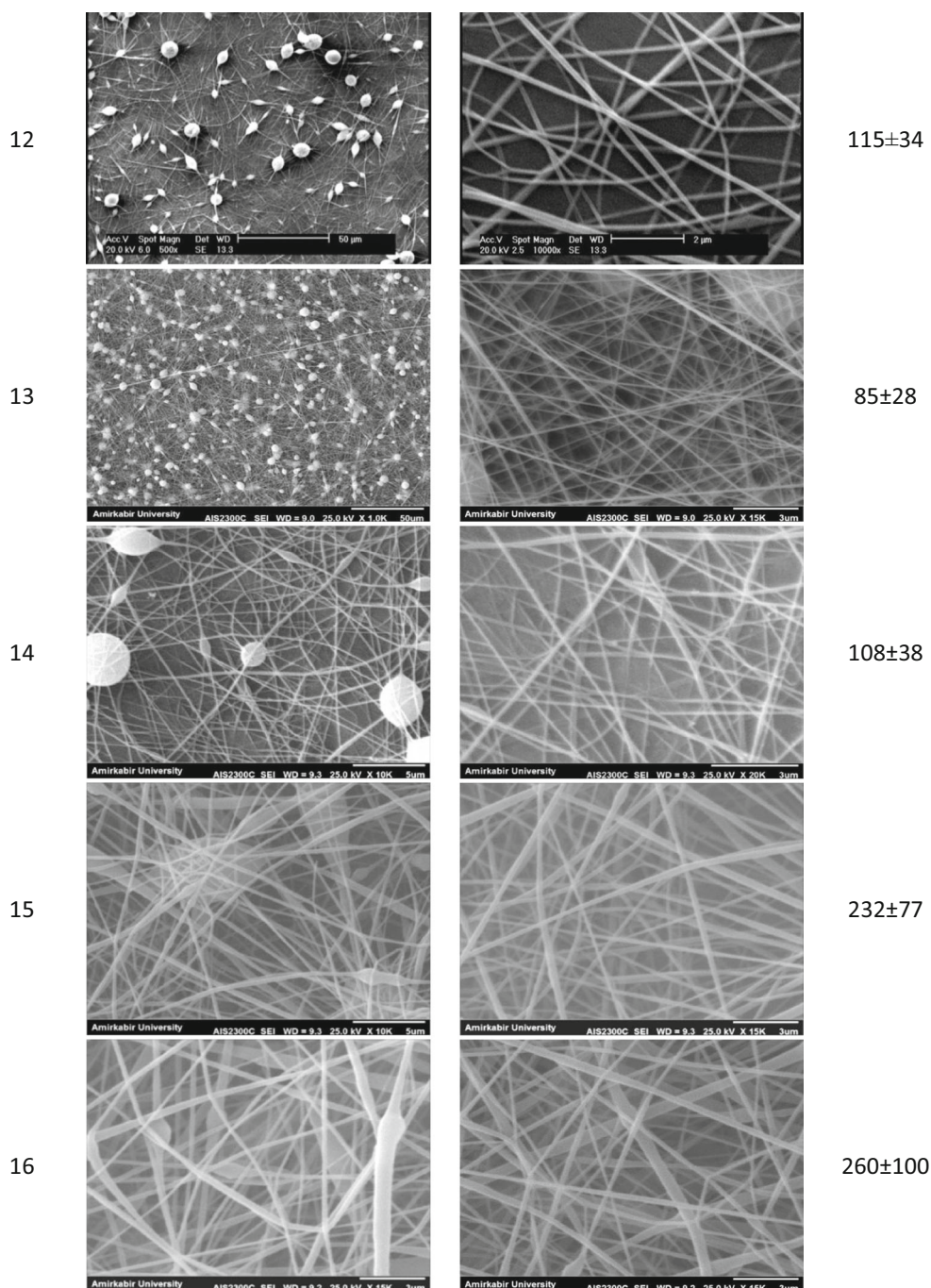


Fig. 3 (continued)

Characterization techniques

Crystalline structure of samples (PVDF film and nanofiber mats) were analyzed by XRD (EQUINOX 3000 model, INEL France Co.) using Cu-K α radiation ($\lambda=0.154$ nm), with the generator working at 40 kV and 30 mA. FTIR spectra of PVDF film and nanofibers were recorded by Spectrometer (model: NEXUS 670,

Nicolet Co.) over a range of 400–4,000 cm^{-1} . Melting temperature (T_m), and melting enthalpy (ΔH_m) of PVDF granule and electrospun nanofibers were measured with differential scanning calorimeter (DSC) (model: DSC 2010, TA Instruments.co) at a heating rate of 20 °C/min. The impedance of samples were measured as a function of frequency (70 Hz to 20 KHz) using an impedance analyzer made in AIMS Lab (<http://aims.aut>.

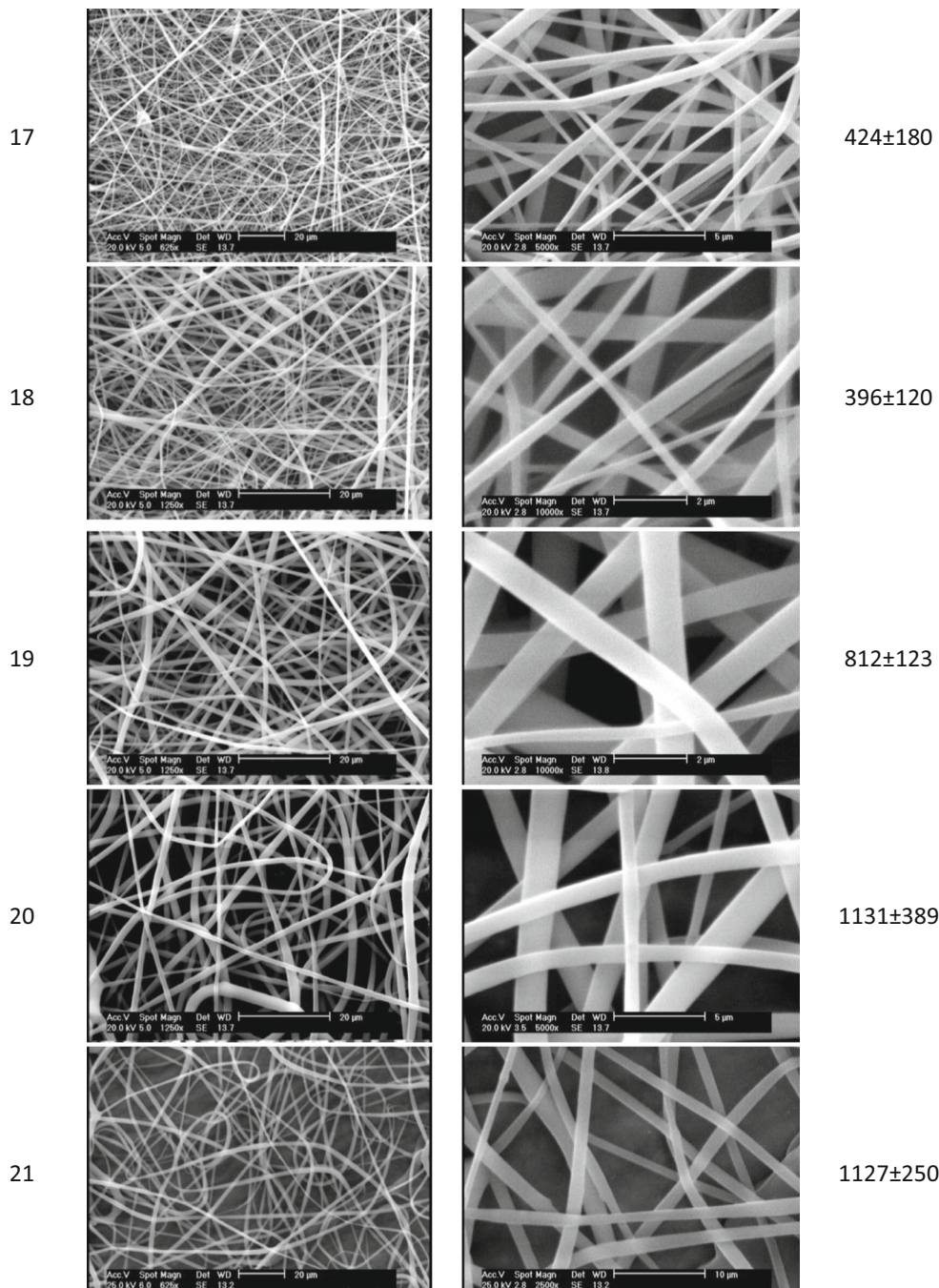


Fig. 3 (continued)

ac.ir/) at room temperature. In order to fabricate the energy conversion device, PVDF nanofiber mat with different thickness (110, 230, 310 μm) with aluminum tape as electrode were used. The aluminum tape was attached to the two sides of the nanofiber mats for measuring output voltage. The thicknesses of mats were measured by a thickness gauge (model: SDLO 34, Shirley Co.). In order to pole of PVDF nanofiber mats obtained from the electrospinning process, the

opposite faces were electrode by attaching thin aluminum tapes with soldered wires. The output of a high voltage power supply (PAD10-25 model, Phenix Co.) was then applied across the terminals coming off the electrode faces. This process of poling was carried out for 4 h at room temperature. To measure the electrical resistance of samples, a Keithley instrument (keithley 2601a) with input voltage between -40 V and +40 V was used. Also, in order to visually detect the

piezoelectric signal from samples, a pressure sensor was fabricated as shown in Fig. 1. A conductive adhesive Aluminum tape (thickness: 0.05 cm), was adhered to the bottom and upper sample, as electrode. The microstructure and the morphology of nanofibers mats was characterized by using scanning electron microscope (SEM, model:XL30,PHILIPS Co.). All samples were gold coated (Bal-tec SCD50 sputter coater) and the images were taken at an acceleration voltage of 20 kV. The fiber diameter was measured using image processing software (ImageJ, National Institutes of Health, USA).

Fabrication of power-generating devices

To fabricate a nanofiber power generator, a small piece of PVDF nanofiber mat (2 cm^2) was used as an active layer. A paper tape frame was set just outside the nanofiber mat and this help to keep away from environmental noises effectively. Two pieces of thin aluminum tape were used as electrodes which sandwiched the PVDF nanofiber mat and placed on the collector. The whole device was then sealed using a commercial paper tapes (Fig. 2).

Measuring output voltage of electrospun fibrous devices

Experimental setup for measuring the output voltage of samples ($2\text{ cm}\times 1\text{ cm}$) is shown in Fig. 1. The sample with an electrically insulated (electrical tape) top surface to avoid any electrical interference between the stainless steel weight and the sample, was placed on a wooden table. The stainless steel weight was dropped from a fixed height through a paper pipe onto the sample. The stainless steel weight drop distance was 15 cm and its mass was 5 g. The stainless steel weight was dropped directly onto sample top surface and the output voltage was recorded and display data by data acquisition card Advantech (PCI-1716) and computer

for each sample upon impact by the stainless steel weight.

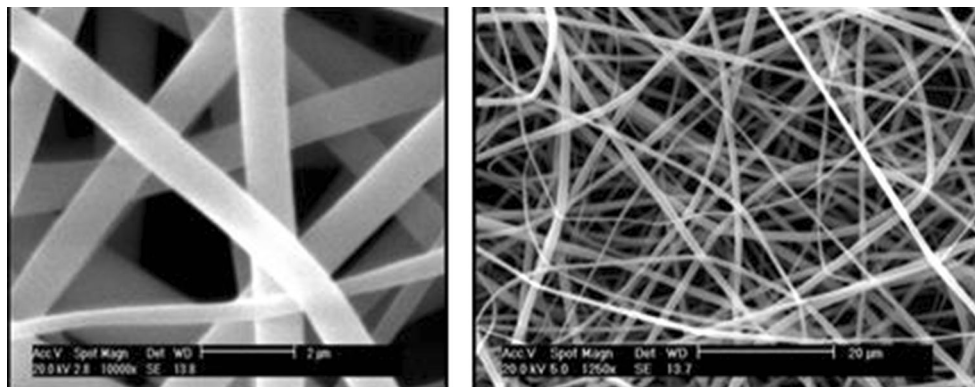
Results and discussions

Optimization the process condition and morphological study of the electrospun PVDF nanofiber membranes

The SEM images (at two different scales except for sample No. 2, 3 and 4 because no fiber was formed) and mean fiber diameter of electrospun PVDF nanofiber (according to Table 1) are shown in Fig. 3. As it is clear from Fig. 3, non-uniform nanofibers with different defects such as beads, and solution spray dots were produced in some process conditions suggesting that solution or process parameters are not suited to make a uniform jet during the electrospinning.

SEM images in Fig. 3 show that with using the rotating collector and increasing feed rate nanofibers can be formed (comparison sample No.1 with 2, 3, and 4). Also with comparison of the SEM images No.5 and 12, generally it can be seen that an increase in solution concentration with applied voltage (above 15 kV) nanofibers with more uniform structure can be fabricated (decreasing size of bead, with decreasing diameter). Pervious researches showed that increasing the concentration of polymer is a key parameter in order to produce nanofibers without bead [26]. Increasing applied voltage and adding a solvent with low boiling point into the electrospinning solutions, can result increases in β -phase contents in nanofibers, and consequently, increase piezoelectric response [18, 19]. It can be also easily confirmed that with an increasing in concentration of polymer solution (keeping other parameters constant) the average fiber diameter increases. The larger fiber diameters at high concentrations could be attributed to the viscosity of the solution that could be high enough to lower the bending instability of the jet

Fig. 4 SEM images at two different scales for the optimized sample with uniform fibers



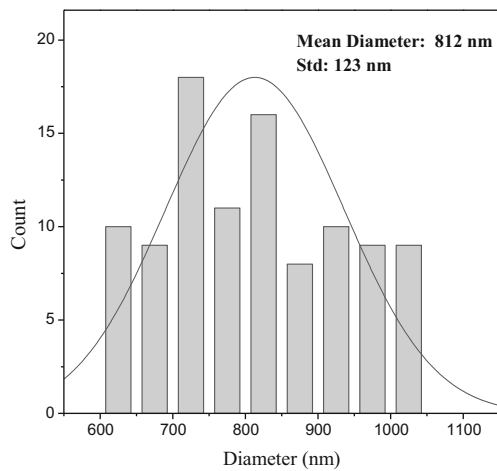


Fig. 5 Histogram of fiber diameter distribution for the optimized sample

and consequently, decreasing the drawing forces in the spinning zone [27–33].

Comparing the SEM images of samples No. 13 and 14 with samples No. 15 and 16, it can be concluded that with considering the concentration to applied voltage ratio for two samples (No.13, 14) with samples (No.15, 16) is almost the same, in the volumetric ratio of 6 to 4 solvents (DMF to acetone), nanofibers with more bead defects have been produced. This could be due to the fact that, in lower acetone/DMF ratio, evaporation rate of solvents during electrospinning process is reduced, and therefore, the polymer droplet imposes more stretch ratio to the jet before reaching to the collector [18], although the influence of increasing polymer concentration should not be neglected. Comparing the SEM images of samples No.17 (without rotating speed) and 18 (with rotating), the influence of rotating collector in order to produce uniform electrospun fibers

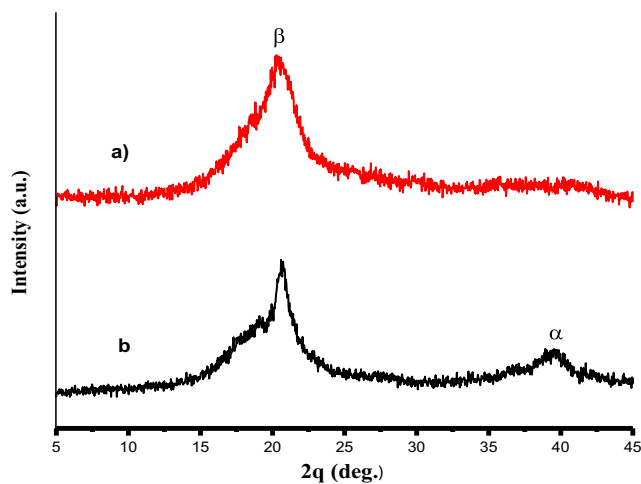


Fig. 6 X-ray diffraction patterns for a) electrospun PVDF nanofiber mats; b) PVDF film

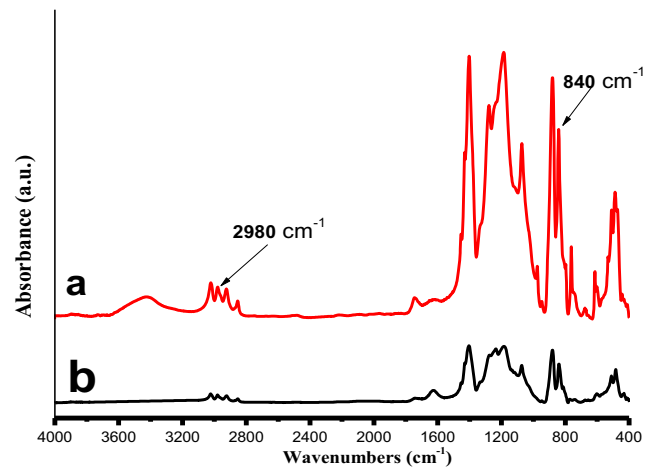


Fig. 7 FTIR spectra: a) electrospun PVDF nanofiber mats; b) PVDF film

without beads can be considerable. Based on these results, following parameters were selected for fabrication of the nanogenerator device: 6/4 (DMF/acetone) volume ratio of solvents, 20 kV of applied voltage, and 23 wt. % of polymer concentration. SEM images at different scale and fiber diameter distribution for the optimized sample (No. 19) are shown in Figs. 4 and 5, respectively. As it is shown in Fig. 4, fibers are uniform in their longitudinal axis which is in high interest for sensor and/or actual applications. In these applications there is a need for getting a constant response from each part of the membrane.

X-ray diffraction analysis

Since to create the piezoelectric properties in electrospun PVDF nanofiber mats, the β-phase crystalline should be formed which is the one with the most effective

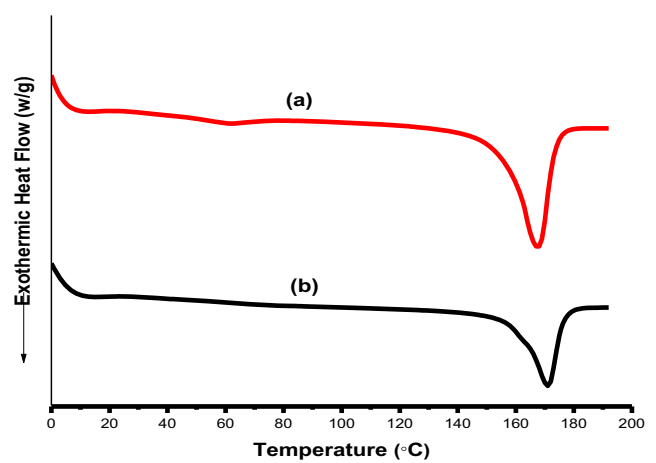
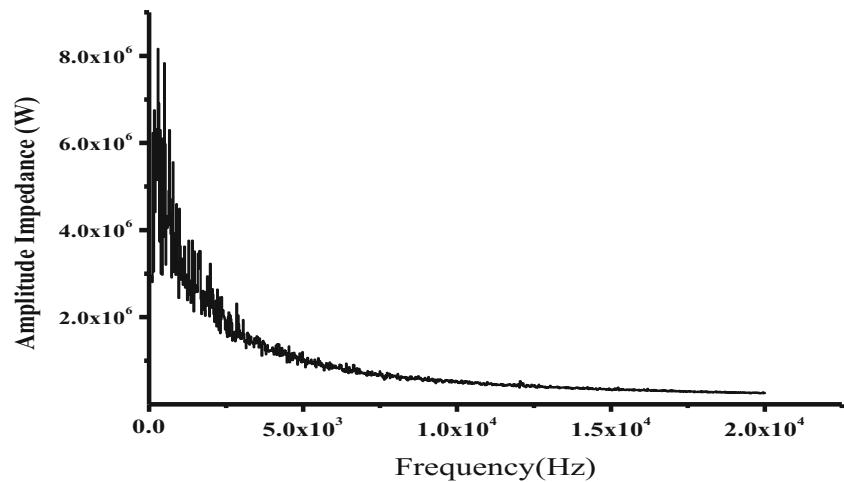


Fig. 8 DSC thermograms: a) electrospun PVDF nanofiber mats; b) PVDF granules (with heating rate of 20 °C/min)

Fig. 9 The experimental amplitude impedance of piezoelectric electrospun PVDF fibrous device as a function of frequency at room temperature



piezoelectricity, X-ray diffraction (XRD) of the optimized sample was performed. XRD patterns provide information on the long-range order and the crystal structure of random networks. As shown in Fig. 6, the XRD curves show a typical β crystal phase peak at around $2\theta=20.5^\circ$, which is assigned to the total diffraction in (110) and (200) planes [10, 34–36]. The peak at 40° corresponds to the reflection of the (020) plane of the α -phase. This peak (α -phase) reduced in intensity for electrospun membrane compared to the PVDF films produced with DMF solvent. This suggests that less α -phase and more β -phase is formed during the electrospinning [34]. Therefore, the electrospinning processes can be effectively utilized to formation of β -phase crystalline and improved piezoelectric properties in nanofiber mats. This could be attributed to the fact that the application of high voltages in the electrospinning process essentially leads to the alignment of the electric dipoles present in the PVDF solution, with the degree of

alignment being proportional to the magnitude of the applied electric field.

Fourier transform infrared spectroscopy (FTIR) analysis

The FTIR spectrum of the nanofiber mats shows vibration peaks at 840 cm^{-1} and $1,280\text{ cm}^{-1}$ (Fig. 7), which are typical vibration characteristics of the β crystalline phase according the previous research and finding [10, 16, 34–37].

The content of β -phase was characterized by the absorbance ratio, A_β , of the FTIR absorption peaks at 840 cm^{-1} and peaks at $2,980\text{ cm}^{-1}$ based on the Eq. (1) [38].

$$A_\beta = \frac{A_{840}}{A_{2980}} \quad (1)$$

where A_{840} and A_{2980} represented the FTIR absorbance peak height at 840 cm^{-1} (characteristic of β -phase) and

Fig. 10 The experimental electrical resistant of the electrospun PVDF nanofiber mats

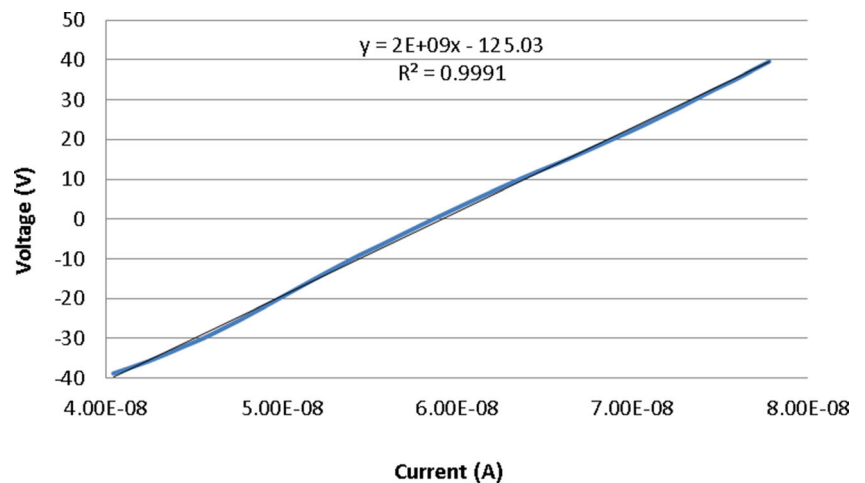
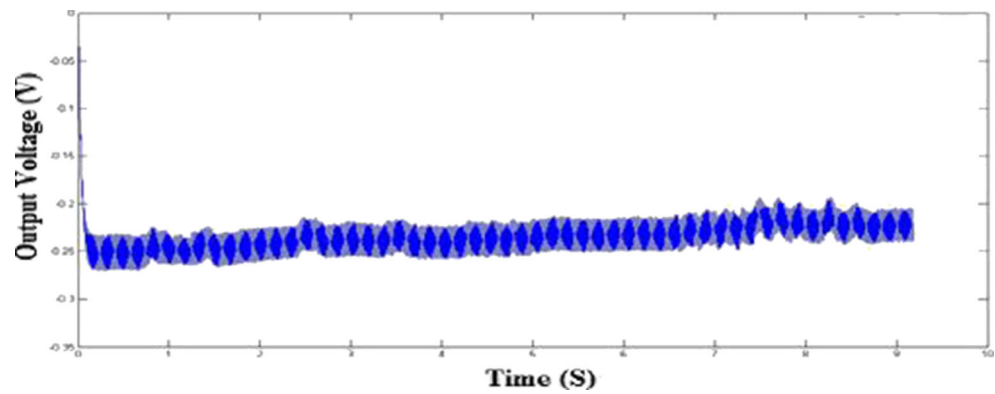


Fig. 11 Output voltage of sample without poling treatment



2,980 cm^{-1} respectively. By contrast, the bands of the non-polar α -phase are not appreciable, which confirmed the results obtained from XRD. Furthermore, the β crystal phase content, $F(\beta)$, in the nanofibers was estimated based on the Eq. (2) [36]. For the nanofibers prepared using the electrospinning, the β crystal phase content increased from 11 % for the PVDF film sample to 68 % for electrospun PVDF nanofibers.

$$F(\beta) = \frac{A_\beta}{1.26A_\alpha + A_\beta} \tag{2}$$

where A_α and A_β are the absorbance at 763 and 840 cm^{-1} .

From XRD and FTIR results revealed that the film has a weaker β -phase crystallines than electrospun nanofibers mats. Therefore this can be conferred that for create piezoelectric properties, electrospinning processing brings the formation of β -phase crystalline in PVDF membrane without need to post treatment (e.g. drawing, annealing and etc.).

DSC analysis

Figure 8 presents DSC melting traces of electrospun PVDF nanofiber mats and granules. The melting temperature (T_m) of PVDF granules (170.96 $^\circ\text{C}$) is more than nanofibers (167.45 $^\circ\text{C}$). The crystalline structure at the higher temperature region is the sign of formation of the α -phase while that at the lower one is the β -phase [39] and the melting point of β -phase is less than the melting point of α -phase [35]. It can also be seen from Fig. 8 that the melting enthalpy of PVDF nanofibers ($\Delta H_m=68.22\text{j/g}$) is much more than granules (41.70 J/g). As a result, according to Eq. (3) [39], there is an increase in crystallinity for electrospun nanofiber mats (for granules is around 40 % and for nanofibers is 65 %), which that confirmed formation a new

crystalline structure (e.g. β phase) in electrospun nanofiber mats.

$$X_C = \frac{\Delta H_m(\text{sample})}{\Delta H_m(\text{lit})} * 100, (\Delta H_m(\text{lit}) = 104.7\text{j/g}) \tag{3}$$

which $\Delta H_m(\text{lit})$ is enthalpy of melting for 100 % crystalline material.

Measuring electrical properties

Amplitude impedance

Amplitude impedance via applying frequency by using impedance analyzer is shown in Fig. 9. This behavior indicates that the piezoelectric device (consist of nanofiber mats and two aluminum tape electrode) has an acceptable capacitance property.

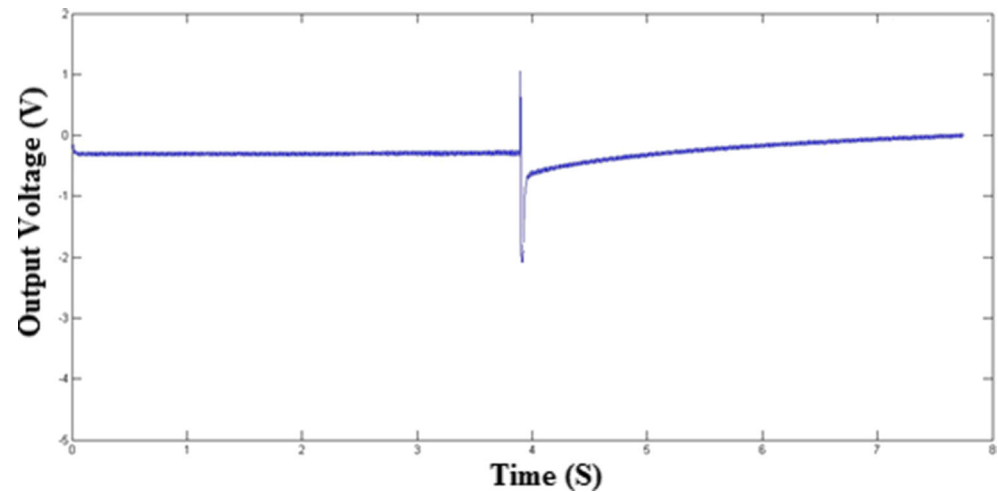
Electrical resistant of electrospun PVDF fibrous mats

The electrical resistance of the fibrous structure was measured with Keithley instrument. As it can be seen in Fig. 10, the order of electrical resistance of electrospun PVDF nanofiber mats is Giga ohms (around 2 $\text{G}\Omega$).

Table 3 Five repeat of the output voltages (pick to pick) for each sample at different thicknesses

Measured Voltage (V)	Thickness(μm)		
	110	230	310
Repeat 1	3.3	5.5	6.4
Repeat 2	3.2	5.4	6.2
Repeat 3	3.1	5.2	6.1
Repeat 4	2.9	5.1	5.9
Repeat 5	2.8	5	5.9
Average value	3.06	5.24	6.1

Fig. 12 Voltage output of the device with 110 μm nanofiber mat's thickness



Piezoelectric performance of the fabricated device (voltage output)

Voltage outputs generated by impact effect were detected by an experimental setup as it is shown in Fig. 11. Piezoelectric response of initial electrospun PVDF fibrous mats as shown in Fig. 11 is not desirable and detectable. This could be due to random orientation of micro-nanofibers within the mat structure of the device, which causes neutralization of electric dipoles of each other.

Therefore, in order to pole the electrospun nanofiber mats, the opposite faces of samples were electroded by attaching thin aluminum tapes with soldered wires. A high voltage of 1.2, 2.6, and 3.9 kV were applied through the terminals coming off from the electroded faces for samples with thicknesses 110, 230 and 310 μm , respectively, using a DC power supply (PAD10-25). This process of poling was carried out for

4 h. The output voltage (pick to pick) for electrospun PVDF micro-nanofibers mats with different thicknesses was measured for each sample with 5 time repeats and the mean value used for interpretations (Table 3). Typical output voltage diagrams for samples with thicknesses of 110, 230, and 310 μm are shown in Figs. 12, 13, 14, respectively. Also to make ensure that voltage output is only arisen from electrospun PVDF nanofiber mats, an electrospun PVA mat with the same thickness (120 μm) was used instead of PVDF nanofiber mat within the device and then voltage output was measured. The result showed no signal voltage output from PVA sample as it was expected.

In order to investigate the effect of pure thickness on the output voltage of the device, results were normalized to thickness for each sample (Table 4). It was interestingly found that normalized output voltage decreases with increasing the thickness of electrospun nanofiber mats. This could be due to the

Fig. 13 Voltage output of the device with 230 μm nanofiber mat's thickness

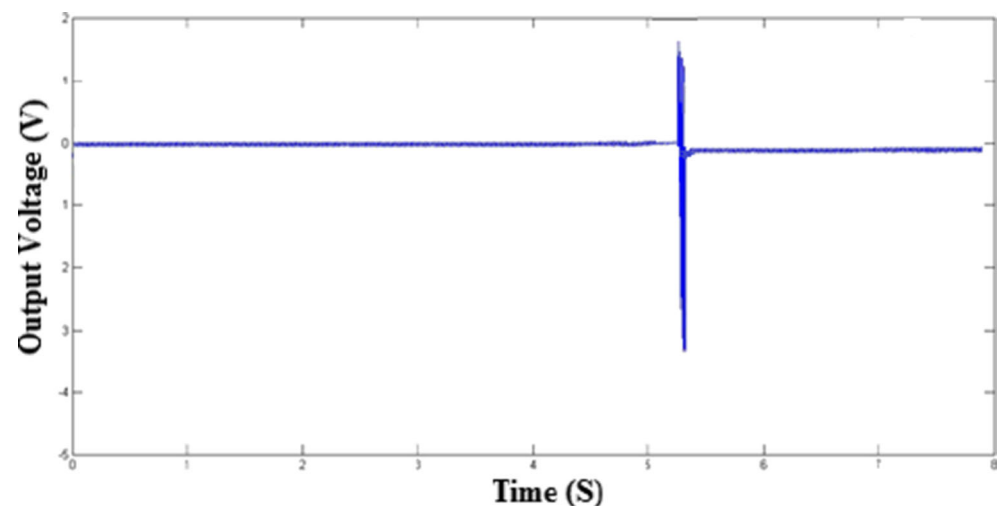
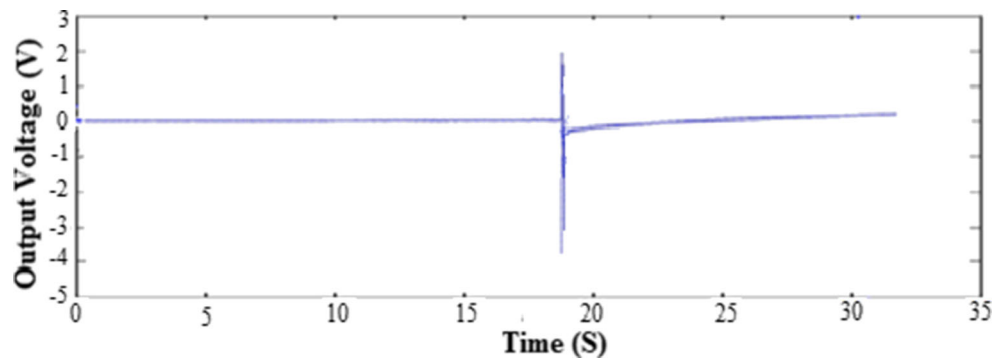


Fig. 14 Voltage output of the device with 310 μm nanofiber mat's thickness



fact that with increasing the thickness of mats, fibers within the structure of samples can be more randomly oriented which causes neutralization of electric dipoles of each other.

Conclusions

In this work, an attempt was made to explore the possibility of utilizing a fabrication scheme for developing a one-step electrospun nanofiber-based mechanical-to-electrical generator. The possible mechanism for the formation of β-phase PVDF produced by electrospinning might be attributed to several factors including: nucleation of the β-phase due to the high applied voltage, and high stretching ratio to the droplets during the electrospinning process which is in some way similar to uniaxial mechanical stretching and poling treatments. A one-step fabrication process of piezoelectric PVDF nanofiber mat that can be used to convert mechanical energy to electrical power was tested successfully in this research. Voltage outputs were obtained as high as several volts and the electrical energy was able to be stored to power electronic devices. It has been also revealed that several factors, including the polymer solution parameters, geometry of the collector, electrospinning parameters and materials of the electrodes, should be taken into account in designing and fabricating the efficient devices for using in the smart and wearable electronic textiles applications. This nanofiber mat

power generating device may provide a simple, efficient, cost-effective and flexible solution to self-powering of microelectronics textiles for various purposes.

Results also showed that in spite of the existed literature, increases in the thickness of nanofiber membranes can lead to decrease the output voltage of nanogenerator which can be considered for further investigations.

Acknowledgments The support provided by the ATMT Research Institute, Amirkabir University of Technology and INSF (Grant No. 91051749) are highly appreciated.

References

1. Tang SLP (2009) Recent developments in flexible wearable electronics for monitoring applications. *Trans Inst Meas Control* 29:283–300
2. Huang C-T, Tang C-F, Lee M-C, Chang S-H (2008) Parametric design of yarn-based piezoresistive sensors for smart textiles. *Sensors Actuators A Phys* 148(1):10–15
3. Stylios GK (2007) SMART textiles special issue. *Trans Inst Meas Control* 29:213–214
4. Persano L, Dagdeviren C, Su Y, Zhang Y, Girardo S, Pisignano D et al (2013) High performance piezoelectric devices based on aligned arrays of nanofibers of poly(vinylidene fluoride-co-trifluoroethylene). *Nat Commun* 4:1633. doi:10.1038/ncomms2639
5. DODDS JS (2012) Development of Piezoelectric Zinc Oxide Nanoparticle-Poly(Vinylidene Fluoride) Nanocomposites for Sensing and Actuation: CALIFORNIA
6. Fang J, Wang X, Lin T (2012) Power generation from randomly oriented electrospun nanofiber membranes. *Adv Mater Res* 479–481: 340–3
7. Harrison JS, Ounaies Z (2001) Piezoelectric Polymers. Report No.: 43
8. Chang J, Dommer M, Chang C, Lin L (2012) Piezoelectric nanofibers for energy scavenging applications. *Nano Energy* 1(3):356–371
9. Fang J, Wang X, Lin T (2012) Power generation from randomly oriented electrospun nanofiber membranes. *Adv Mater Res* 479–481: 340–343
10. Fang J, Wang X, Lin T (2011) Electrical power generator from randomly oriented electrospun poly(vinylidene fluoride) nanofiber membranes. *J Mater Chem* 21(30):11088–11091
11. Zeng W, Tao X-M, Chen S, Shang SM, Wong L-WC, Choy SH (2013) Highly durable all-fiber nanogenerator for mechanical energy harvesting. *Energy Environ Sci* 6(9):2631–2638
12. Ant SR, Sodano HA (2007) A review of power harvesting using piezoelectric materials (2003–2006). *Smart Mater Struct* 16:R1–R21

Table 4 Output voltage normalized to the thickness for each sample

Normalized output voltage (V)	Thickness (μm)		
	110	230	310
Repeat 1	0.03	0.023	0.020
Repeat 2	0.029	0.023	0.02
Repeat 3	0.028	0.022	0.019
Repeat 4	0.026	0.022	0.019
Repeat 5	0.025	0.021	0.019
Mean value (V)	0.028	0.023	0.020

13. Lee CS, Joo J, Han S, Koh SK (2004) Multifunctional transducer using poly(vinylidene fluoride) active layer and highly conducting poly (3,4-ethylenedioxythiophene) electrode: actuator and generator. *Appl Phys Lett* 85:1841–1843
14. Kochervinskii VV (2008) Specifics of structural transformations in poly(vinylidene fluoride)-based ferroelectric polymers in high electric fields. *Polym Sci Ser C* 50(1):93–121
15. Fukada E (2000) History and recent progress in piezoelectric polymers. *Ultrason Ferroelectr Freq Control IEEE Trans* 47(6):1277–1290
16. Mandal D, Yoon S, Jin KK (2011) Origin of piezoelectricity in an electrospun poly(vinylidene fluoride-trifluoroethylene) nanofiber web-based nanogenerator and nano-pressure sensor. *Macromol Rapid Commun* 32(11):831–837
17. Chang C, Tran VH, Wang J, Fuh Y-K, Lin L (2010) Direct-write piezoelectric polymeric nanogenerator with high energy conversion efficiency. *Nano Lett* 10(2):726–731
18. Ribeiro C, Sencadas V, Ribelles JLG, Lanceros-Méndez S (2010) Influence of processing conditions on polymorphism and nanofiber morphology of electroactive poly(vinylidene fluoride) electrospun membranes. *Soft Mater* 8(3):274–287
19. Zheng J, He A, Li J, Han CC (2007) Polymorphism control of poly(vinylidene fluoride) through electrospinning. *Macromol Rapid Commun* 28(22):2159–2162
20. Sencadas V, Gregorio R Jr, Lanceros-Méndez S (2009) α to β phase transformation and microstructural changes of PVDF films induced by uniaxial stretch. *J Macromol Sci Part B: Phys* 48(3):514–525
21. Bormashenko Y, Pogreb R, Stanevsky O, Bormashenko E (2004) Analysis Method Vibrational spectrum of PVDF and its interpretation. *Polym Test* 23:791–796
22. Greeshmaa T, Balajia R, Nayakb MM, Jayakumara S (2009) The influence of individual phases on piezoelectric coefficient of PZT-PVdF composites. *Ferroelectrics* 393(1):88–93
23. Gheibi A, Latifi M, Merati AA, Bagherzadeh R (2014) Piezoelectric electrospun nanofibrous materials for self-powering wearable electronic textiles applications. *J Polym Res* 21:469
24. Hansen BJ, Liu Y, Yang R, Wang ZL (2010) Hybrid nanogenerator for concurrently harvesting biomechanical and biochemical energy. *ACS Nano* 4(7):3647–3652
25. Gheibi A, Latifi M, Merati A, Bagherzadeh R (2014) Piezoelectric electrospun nanofibrous materials for self-powering wearable electronic textiles applications. *J Polym Res* 21(7):1–7
26. Ramakrishna S, Fujihara K, Teo W-E, Lim T-C, Ma Z (2005) An introduction to electrospinning and nanofibers National University of Singapore: World Scientific Publishing Co. Pte. Ltd.
27. Bagherzadeh R, Shaikhzadeh Najar S, Latifi M, Amani Tehran M, Kong L (2012) A theoretical analysis for fiber contacts in multilayer nanofibrous assemblies. *Text Res J* 18:2012
28. Bagherzadeh R, Latifi M, Shaikhzadeh Najar S, Amani Tehran M, Gorji M, Kong L (2011) Transport properties of multi-layer fabric based on electrospun nanofiber mats as a breathable barrier textile material. *Text Res J* 82(1):70–76
29. Bagherzadeh R, Shaikhzadeh Najar S, Latifi M, Amani Tehran M, Kong L (2013) A theoretical analysis and prediction of pore size and pore size distribution in electrospun multilayer nanofibrous materials. *J Biomed Mater Res Part A* 101A(7):2107–2117
30. Bagherzadeh R, Latifi M, Najar SS, Tehran MA, Kong L (2013) Three-dimensional pore structure analysis of Nano/Microfibrous scaffolds using confocal laser scanning microscopy. *J Biomed Mater Res Part A* 101A(3):765–774
31. Bagherzadeh R, Latifi M, Kong L (2014) Three-dimensional pore structure analysis of polycaprolactone nano-microfibrous scaffolds using theoretical and experimental approaches. *J Biomed Mater Res Part A* 102A:903–910
32. Bagherzadeh R, Latifi M, Shaikhzadeh Najar S, Kong L (2014) Experimental verification of theoretical prediction of fiber to fiber contacts in electrospun multilayer nano-microfibrous assemblies: effect of fiber diameter and network porosity. *J Ind Text* 43(4):483–495
33. Bagherzadeh R, Latifi M, Shaikhzadeh Najar S, Amani Tehran M, Kong L (2014) The application of Cd Se/ZnS quantum dots and confocal laser scanning microscopy for three-dimensional imaging of nanofibrous structures. *J Ind Text* 43(4):496–510
34. Parka YJ, Soo Kang Y, Parka C (2005) Micropatterning of semicrystalline poly(vinylidene fluoride) (PVDF) solutions. *Eur Polym J* 41(5):1002–1012
35. Satapathy S, Santosh P, Gupta PK, Varma KBR (2011) Effect of annealing on the phase transition in poly (vinylidene fluoride) films prepared using polar solvent. *Bull Mater Sci* 34(4):727–733
36. Keun Yoon L, Kyu KB (2000) Compatibility of poly(vinylidene fluoride) (PVDF)/polyamide 12 (PA12) blends. *Appl Polym Sci* 78(7):1374–1380
37. Park J-W, Seo Y-A, Kim I, Ha C-S (2004) Investigating the Crystalline Structure of Poly(vinylidene fluoride) (PVDF) in PVDF/Silica Binary and PVDF/Poly(methyl methacrylate)/Silica Ternary Hybrid Composites Using FTIR and Solid-State ^{19}F MAS NMR Spectroscopy. *Macromolecules* 37(2):429–436
38. Xia Q, Zhao XJ, Chen SJ, Ma WZ, Zhang J, Wang XL (2010) Effect of solution-blended poly(styrene-co-acrylonitrile) copolymer on crystallization of poly(vinylidene fluoride). *Express Polym Lett* 4(5):284–291
39. Choia S-S, Lee YS, Joo CW, Lee SG, Park JK, Hanc K-S (2004) Electrospun PVDF nanofiber web as polymer electrolyte or separator. *Electrochim Acta* 50(2–3):339–343